We are IntechOpen,
the world's leading publisher of Open Access books
Built by scientists, for scientists

6,900
Open access books available

185,000
International authors and editors

200M
Downloads

154
Countries delivered to

Our authors are among the

TOP 1%
most cited scientists

12.2%
Contributors from top 500 universities

CLARIVATE ANALYTICS
BOOK CITATION INDEX
INDEXED

WEB OF SCIENCE™

Selection of our books indexed in the Book Citation Index
in Web of Science™ Core Collection (BKCI)

Interested in publishing with us?
Contact book.department@intechopen.com

Numbers displayed above are based on latest data collected.
For more information visit www.intechopen.com

Structural and Functional Aspects of Viroporins in Human Respiratory Viruses: Respiratory Syncytial Virus and Coronaviruses

Wahyu Surya, Montserrat Samsó and Jaume Torres

Additional information is available at the end of the chapter

1. Introduction

Viroporins are an increasingly recognized class of small viral membrane proteins (~60-120 amino acids) which oligomerize to produce hydrophilic pores at the membranes of virus-infected cells [1]. The existence of 'viroporins' was proposed more than 30 years ago after observing enhanced membrane permeability in infected cells [2]. These proteins form oligomers of defined size, and can act as proton or ion channels, and in general enhancing membrane permeability in the host [3]. Even though viroporins are not essential for the replication of viruses, their absence results in attenuated or weakened viruses or changes in tropism (organ localization) and therefore diminished pathological effects [4, 5].

In addition to having one – sometimes two – α-helical transmembrane (TM) domain(s), viroporins usually contain additional extramembrane regions that are able to make contacts with viral or host proteins. Indeed, the network of interactions of viroporins with other viral or cellular proteins is key to understand the regulation of viral protein trafficking through the vesicle system, viral morphogenesis and pathogenicity.

In general, viroporins participate in the entry or release of viral particles into or out of cells, and membrane permeabilization may be a desirable functionality for the virus. Indeed, several viral proteins that are not viroporins are known to affect membrane permeabilization, e.g., A38L protein of vaccinia virus, a 33-kDa glycoprotein that allows Ca^{2+} influx and induces necrosis in infected cells [6]. In viruses that lack typical viroporins, their function may be replaced by such pore-forming glycoproteins. For example, HIV-2 lacks typical viroporins, and ROD10 Env is an envelope glycoprotein that enhances viral particle release. In HIV-1, this function is attributed to the viroporin Vpu [7].

An important point that needs to be established, in view of the observed channel activity of viroporins, is whether the channels they form are selective, with a controlled gating mechanism, or whether permeabilization is non selective, like in some antimicrobial peptides [8]. Viroporins have also been found to modulate endogenous cellular channels [9-12] and this activity may also have an important regulatory role during the life cycle of the virus.

Viroporins can be found in all kinds of viruses, RNA, DNA, enveloped and non-enveloped. Examples of viroporins are picornavirus 2B [13], alphavirus 6K [14-16], HIV-1 Vpu [17, 18], influenza virus A M2, (also called AM2) [19], RSV SH protein [20], p10 protein of avian reovirus [21], Human hepatitis C virus (HCV) and bovine viral diarrhea virus (BVDV) p7 [22, 23], Paramecium bursaria chlorella virus (PBCV-1) Kcv [24], and coronavirus envelope proteins, e.g., SARS-CoV E [25, 26]. Recent reviews [27, 28] provide more examples and possible functional roles.

The most extensively studied viroporin to date is probably the M2 protein from influenza A virus (AM2). AM2 protein is 97-residue long, with one transmembrane (TM) domain and a C-terminal cytoplasmic amphiphilic helix. AM2 forms homotetramers and is located in the viral envelope, where it enables protons from the endosome to enter the viral particle (virion). This lowers the pH inside the viral particle, causing dissociation of the viral matrix protein M1 from the ribonucleoprotein RNP, uncoating of the virus and exposure of the content to the cytoplasm of the host cell. AM2 also delays acidification of the late Golgi in some strains [29, 30].

The proton channel activity of AM2 can be inhibited by antiviral drugs amantadine and rimantadine, which block the virus from taking over the host cell. Two different high-resolution structures of truncated forms of AM2 have been reported: the structure of a mutated form of its TM region (residues 22-46) [31], and a slightly longer form (residues 18-60) containing the TM region and a segment of the C-terminal domain [32, 33]. These studies suggest that the known AM2 adamantane inhibitors, amantadine and rimantadine, act by either blocking the pore [31, 34] or by an allosteric mechanism [32]. New AM2 inhibitors have been reported [35], but their effectiveness against adamantane-resistant viruses remains to be established. The use of these drugs presents a classical example of targeting viral channels to treat viral infection infection [31, 32, 36].

The case of AM2 protein in influenza A represents a link between viroporin activity and structure to viral pathogenesis. Unfortunately, for many viroporins even rudimentary structural models are lacking due to high hydrophobicity, conformational flexibility and tendency to aggregate. For some viroporins however, increasing degrees of structural information can be obtained due to availability of high quality purified protein. Examples of these are the viroporins present in coronaviruses (CoV) and in the respiratory syncytial virus (RSV), envelope (E) protein and the small hydrophobic (SH) protein, respectively. Both types of virus infect the upper and lower respiratory tract of humans, and their viroporins are the subject of this chapter.

2. Envelope (E) and Small Hydrophobic (SH) proteins in respiratory viruses

2.1. SH protein in hRSV

Medical impact of the human respiratory syncytial virus (hRSV) infection. hRSV is a member of the *Paramyxoviridae* family, and is the leading cause of bronchiolitis and pneumonia in infants and the elderly worldwide [37]. hRSV infection is the most frequent cause of hospitalization of infants and young children in industrialized countries. In the USA alone, around 100,000 infants with hRSV infection are hospitalized annually. hRSV also is a significant problem in the elderly, patients with cardiopulmonary diseases and in immunocompromised individuals. hRSV accounts for approximately 10,000 deaths per year in the group of >64 years of age in the US. Globally, hRSV infection results in 64 million cases and 160,000 deaths every year (http://www.who.int/vaccine_research/diseases/ari/en/index2.html).

There is currently no effective vaccine available to prevent hRSV infection. Development of vaccines has been complicated by the fact that host immune responses appear to play a significant role in the pathogenesis of the disease [38]. Naturally acquired immunity to hRSV is neither complete nor durable, and recurrent infections occur frequently during the first three years of life. Palivizumab, a humanized monoclonal antibody directed against hRSV surface fusion F protein (Synagis, by MedImmune), is moderately effective but very expensive. It is currently available as prophylactic drug for infants at high risk. Cost of prevention limits its use in many parts of the world. The only licensed drug for use in infected people is ribavirin, but its efficacy is limited. Antibodies against both F (fusion) and G (attachment) proteins have been found in the serum of hRSV infected patients, but only provide temporary protection. Therefore, low immunoprotection and lack of suitable antivirals leads towards the search and characterization of new drug targets for the effective treatments of hRSV infection. A possible suitable target is the SH protein as will be elaborated below.

The viral particle formation in RSV. Based on the reactive patterns to monoclonal antibodies, there are two hRSV strains that co-circulate in human populations, subtypes A and B. The hRSV genome comprises a nonsegmented negative-stranded RNA of ~15 kb that transcribes 11 proteins, including the three membrane proteins fusion (F), attachment (G), and small hydrophobic (SH) [39, 40]. The F protein is sufficient for mediating viral entry into cells *in vitro*, and the G protein plays a role in viral attachment [41, 42]. In contrast, the precise role of SH protein is still unclear.

hRSV also contains six internal structural proteins: the matrix (M) protein, which provides structure for the virus particle, nucleoprotein (N), phosphoprotein (P) and large (L) polymerase protein form the ribonucleoprotein (RNP) complex, which encapsidates the RSV genome and functions as the RNA-dependent RNA polymerase. Lastly, two isoforms of matrix protein 2 (M2-1 and M2-2) are accessory proteins that control transcription and replication [43]. Viral proteins traffic to the apical surface of polarized epithelial cells, where they

assemble into virus filaments at the plasma membrane [44], although the mechanisms that drive assembly into filaments and budding are not well understood.

Generation of nascent hRSV genomic RNA appears to occur in discrete cytoplasmic inclusion bodies that contain the hRSV N, P, L, M2-1 and M2-2 proteins but not the F, G, or SH proteins [45]. It is suspected that the RNP complexes form in the inclusions and then traffic to the apical membrane, where they meet with the surface glycoproteins F, G, and SH arriving from the Golgi apparatus through the secretory pathway [46]. hRSV proteins and viral RNA assemble into virus filaments at the cell surface. These filaments are thought to contribute to cell-cell spread of the virus and morphologically resemble the filamentous form of virions seen in electron microscopy (EM) studies of virus produced in polarized cells [47].

The small hydrophobic (SH) protein. The SH protein is 65 or 64 amino acids long, in subtype A or B, respectively. SH protein has a single membrane-spanning hydrophobic region [48], and a C-terminal extramembrane tail, oriented extracellularly/lumenally [48]. The sequence of SH protein is highly conserved, especially at the TM domain [49, 50]. hRSV that lacks SH protein, hRSVΔSH, is still viable, and still forms syncytia [51-53]. However, hRSVΔSH was attenuated in *in vivo* mouse and chimpanzee models [4, 5], which indicates that SH protein is important for hRSV pathogenesis. SH protein has been suggested to play an ancillary role in virus-mediated cell fusion [54, 55]. Also, the presence of SH protein has been shown to reduce cytopathic effect (CPE) and apoptosis in L929 and A549 (lung epithelial cell line) infected cells, at least in part by inhibiting tumor necrosis factor α (TNF-α) production [56], similarly to parainfluenza virus 5 (PIV5).

Interaction of SH protein with viral and host proteins. Extensive protein-protein interactions have been observed between the three membrane proteins on the hRSV envelope, F, G, and SH [51, 57, 58] and these interactions have an effect on fusion activity of hRSV on the host [51, 54]. In cells transiently expressing hRSV membrane proteins, the presence of G and SH proteins enhanced fusion activity mediated by F protein [54, 55]. Thus, SH protein has been suggested to play an ancillary role in virus-mediated cell fusion. However, using virus-infected cells the presence of G protein alone enhanced F-mediated fusion activity [51], whereas SH protein in the absence of G protein inhibited it, suggesting a possible interaction between SH and G [51]. Viruses where the SH protein gene was deleted grew better in HEp-2 cells [55], leading to the suggestion of a negative regulatory effect of SH protein on virus-induced membrane fusion, although direct interaction between SH protein and fusion-responsible F protein has not been observed [58], whereas complexes F-G and G-SH have been detected on the surface of infected cells using immunoprecipitation [58] and heparin agarose affinity chromatography [57]. These three proteins not only form hetero-oligomers, but also homo-oligomers: F forms trimers [59], G forms tetramers [60], and SH forms pentamers [48, 61, 62]. Thus, a complicated regulatory network of interactions may exist which probably includes both homo- and hetero-oligomeric forms.

In addition to interactions with viral proteins, the fact that SH proteins of hRSV and parainfluenza virus 5 (PIV5) are necessary for the inhibition of tumor necrosis factor alpha (TNF-α)-induced apoptosis [56, 63] also suggests a possible interaction with host proteins, although this has not been confirmed experimentally. However, in another study,

deletion of SH protein gene from RSV did not result in increased apoptosis in infected H441 cells [11].

Localization and post-translational modifications of SH protein during viral infection. In infected cells, some SH protein is found in plasma membrane and cytoplasm, but most of the SH protein accumulates at the membranes of the Golgi complex and only very low amounts are found in the viral envelope [64]. Several forms of the SH protein, glycosylated and non-glycosylated, are present during infection [65], but the non-glycosylated form appears to be the most abundant [66]. SH protein is also modified by tyrosine phosphorylation [61], and increased accumulation of SH in the Golgi complex was observed in the presence of a kinase inhibitor. Thus, SH protein is modified by a MAPK p38-dependent tyrosine kinase activity and this modification influences its cellular distribution. Although SH contains one cysteine residue, no palmitoylation has been detected in SH protein in conditions where F and G were palmitoylated [48].

Structural determination of SH protein. An important step towards the understanding of viroporin function at the molecular level is the availability of these proteins in a highly pure form. This has been so far difficult due to their high hydrophobicity, toxicity to expression hosts, and tendency to aggregate. However, recently we have been able to obtain the full length SH protein [67] that allows structural and biophysical studies (Fig. 1A).

SH protein after cross-linking has been shown to form multiple oligomers of increasing size in SDS [66, 68]. Later, we showed that the TM domain of SH protein forms only homopentamers in perfluoro-octanoic acid (PFO) gels [69]. Reports using purified full-length SH protein have confirmed the pentameric nature of the oligomer formed by this protein. For example, a bundle formation of a tagged SH protein construct was visualized under electron microscopy and was interpreted as a pentameric or a hexameric structure [70]. Using a purified tag-free SH protein, we have unequivocally demonstrated the homo-pentameric nature of these oligomers in a variety of detergents using analytical ultracentrifugation and electrophoresis (Fig. 1) [71]. Indeed, in the presence of PFO (Fig. 1B) and a variety of other detergents under Blue-native gel electrophoresis (Fig. 1C), the full-length SH protein migrates as a single band with a molecular weight ~40 kDa, consistent with a pentameric oligomer. The pentameric form of SH has been further confirmed by analytical ultracentrifugation sedimentation equilibrium in detergents DPC, C14SB and C8E5 micelles. In these detergents, the species distribution profiles show a best fit to a monomer-pentamer self-association model (Fig. 1 D-E).

Secondary structure of SH protein. The SH protein is predicted to have an α-helical region spanning residues 16-46, which includes its predicted TM region (residues ~20-40, Fig. 1A). Fourier Transform infrared (FTIR) data for the full-length SH protein reconstituted in model lipid bilayers shows the presence of ~60% α-helical structure, whereas the rest is β-structure [71]. The availability of purified, isotopically labeled protein allowed us to obtain a model for this pentameric oligomer where SH protein was reconstituted in DPC micelles using NMR (Fig. 2). The model shows the lumen of the hypothetic channel, sufficient for the passage of ions.
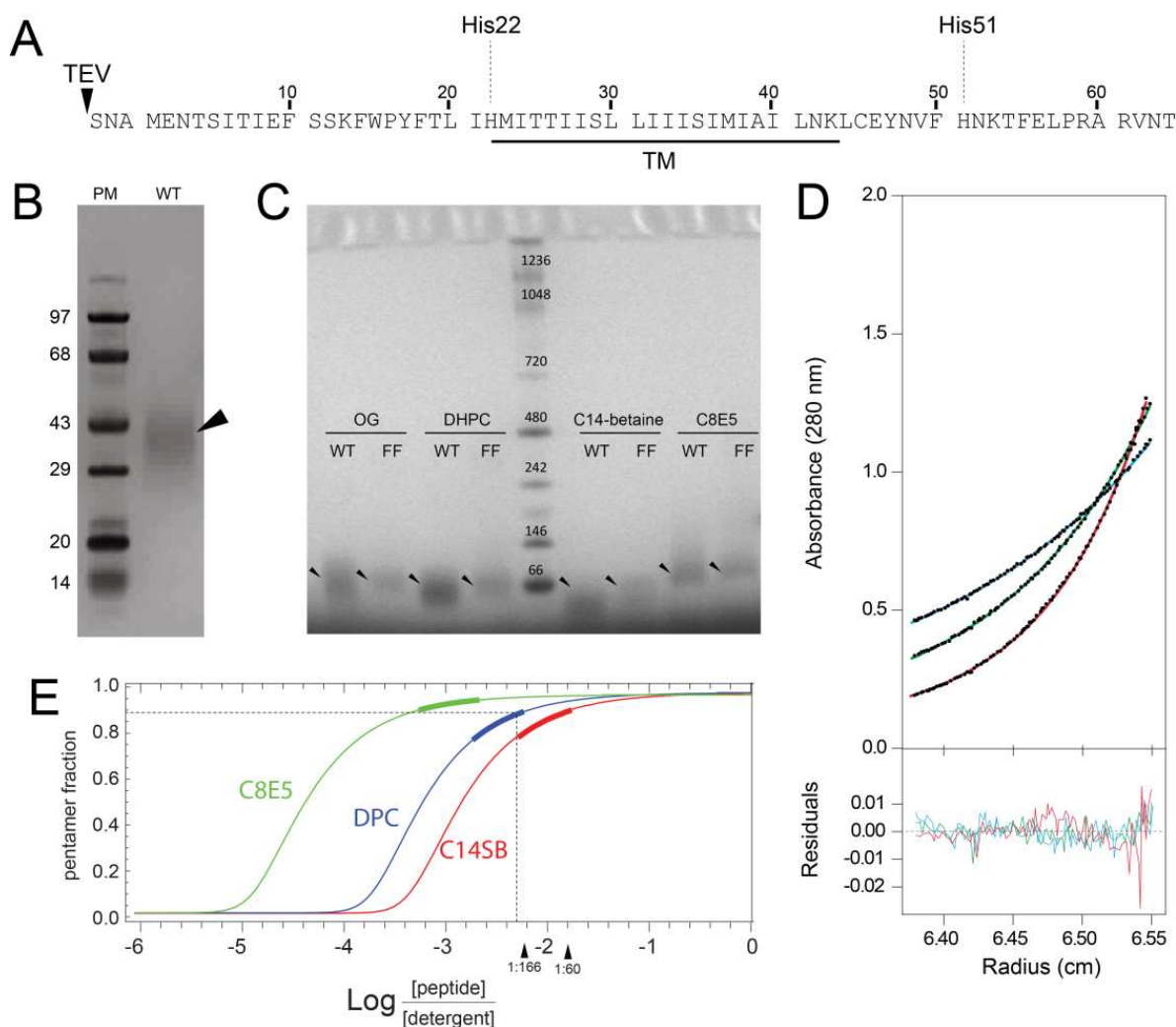
Figure 1. Sequence and oligomerization of SH protein from hRSV subtype A. (A) Amino acid sequence of full-length SH protein, with three additional N-terminal residues, SNA, as a result of tobacco etch virus (TEV) protease cleavage to remove the expression tag [71]; (B) Gel electrophoresis analysis of SH protein in PFO shows a band consistent with pentamers (arrow); (C) Blue-native gel electrophoresis of wild type SH protein (WT) and double mutant H22F/H51F (FF) presolubilized in a variety of detergents show one band migrating consistent with pentamers (arrows); (D) Analytical ultracentrifugation sedimentation equilibrium data for 50 µM SH (WT) protein collected at three different speeds: 16,000 (blue), 19,500 (green), and 24,000 (red) rpm. Sedimentation profile was globally best-fitted to a monomer-pentamer equilibrium model. The graph shows both data points (black filled circles) and fitted function (in color). Lower panels represent fit residuals; (E) SH (WT) oligomeric species distribution in C14SB, C8E5 and DPC detergents, where the thick bar on the curve represents the range of protein:detergent molar ratios used in the AUC experiment. The dotted line indicates the protein:DPC molar ratio (1:200) used in the NMR experiments [71] and its corresponding pentamer fraction (~90%). C14SB, DPC and C8E5 detergent concentrations were 5, 15 and 33 mM, respectively.
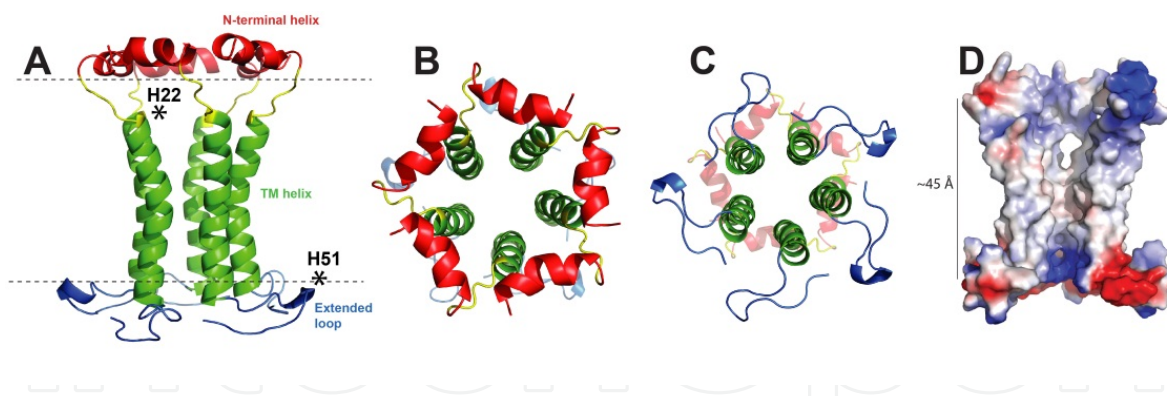
Figure 2. NMR-based pentameric model of RSV SH protein in detergent DPC micelles [71]. (A) Side view; (B) N-terminal (cytoplasmic) view; (C) C-terminal (extracellular or lumenal) view; (D) Electrostatic surface of the assembly showing the mostly hydrophobic central lumen. The SH protein assembly spans the entire bilayer with an overall length of about 45 Å.

Ion channel activity of SH protein. The presence of SH protein at the plasma membrane of HEK293 transfected cells allowed the study of SH protein channel activity [71], which was reported to be pH sensitive. Mutants where both histidines, H22 and H51 (Fig. 1A), were changed to phenylalanine (FF mutant, Fig. 1C), were found to be channel inactive. In a Blue-native gel electrophoresis, this FF mutant showed similar electrophoretic mobility (Fig. 1C) and similar plasma membrane localization to the wild type [71], which suggests that the observed channel activity is not mediated by direct or indirect interaction of SH protein with host-endogenous channels.

One of the two histidines, His22, was suggested to face the lumen of the pentameric oligomer using site-specific infrared dichroism of the isotopically labeled TM domain reconstituted in model lipid bilayers [69]. In the NMR based model of the full length protein (Fig. 2), although His22 adopts a lumenal orientation, the second histidine, His51, appears in an extra-membrane location, at the tip of the C-terminal extended loop (Fig. 2A), which is difficult to reconcile with an activation role based on His protonation. Thus, it is possible that the structure of this C-terminal domain in detergent micelles, used for the NMR experiment, does not represent accurately the structure of SH protein in lipid bilayers, where we obtained the patch clamp data. Nevertheless, the pH-activated channel activity observed, and the histidine-less inactive mutant strongly suggests that protonation of histidines may be involved in channel activity. Indeed, the presence of a lumenal histidine sidechain is reminiscent of the one found in the TM domain of the influenza A AM2 proton channel, which is also activated at low pH via histidine protonation [33].

Despite the similarities between AM2 and SH protein, we have been unable to observe strong proton channel activity of SH protein *in vitro* (unpublished observations). In addition, the different life cycle of hRSV and influenza virus A does not provide a rationale for this hypothetic proton channel activity. Equally, no obvious rationale can be assigned to pH mediated activation. The use of specific channel inhibitors for SH protein could contribute to clarify the precise role of channel activity in this protein, disentangled from other effects.

2.2. E protein in coronaviruses

Medical impact of coronaviruses. Coronaviruses (family *Coronaviridae*, genus *Coronavirus* [72]) are enveloped viruses that cause common cold in humans and a variety of lethal diseases in birds and mammals [73]. The species in the genus *Coronavirus* have been organized into 3 groups with genetic and antigenic criteria [74]: α-coronaviruses include the porcine *Transmissible gastroenteritis virus* (TGEV) and *Human coronaviruses 229E* (HCoV-229E) or NL63 (HCoV-NL63). β-coronaviruses include *Murine hepatitis virus* (MHV) and *Human coronavirus OC43* (HCoV-OC43). γ-coronaviruses include the avian *Infectious bronchitis virus* (IBV) and the Turkey coronavirus (TCoV). The virus responsible for the severe acute respiratory syndrome (SARS-CoV), a respiratory disease in humans, is close to the β-coronaviruses, formerly group 2 [75].

SARS produced a near pandemic in 2003, with 8,096 infected cases and 774 deaths worldwide (fatality rate of 9.6%). Mortality was 6% for those aged 25-44, 15 % for the 45-64 group and >50% for those over 65 (*http://www.who.int/csr/sarsarchive/2003_05_07a/en/*). For comparison, the case fatality rate for influenza A is usually around 0.6% (primarily among the elderly) and 33% in locally severe epidemics of new strains. SARS-CoV was enzootic in an unknown animal or bird species, probably a bat [76], before suddenly emerging as a virulent virus in humans. A similar crossing of the animal-human species barrier is thought to have occurred between the bovine coronavirus (BCoV) and human coronavirus OC43 (HCoV-OC43) more than 100 years ago [77]. Such interspecies jumps, from animal hosts to humans, are likely to reoccur.

Protective efficacy of candidate vaccines against coronaviruses in humans has been mainly studied in animals so far, and only few vaccines have entered Phase 1 human trials [78]. Ribavirin [79], interferons [80], unconventional agents [81-83] and non-steroidal anti-inflammatory agents [84] have shown activity against SARS-CoV and HCoV-229E, but there is no data from animal studies or clinical trials [85]. Studies of antiviral therapy against coronaviruses other than SARS-CoV have been scarce; *in vitro* data show that several chemicals may have inhibitory activities on HCoV-NL63 and HCoV-229E [86, 87].

In addition to the genes involved in viral RNA replication and transcription, other essential genes in coronaviruses encode the common viral structural proteins, S (spike), E (envelope), M (membrane) and N (nucleocapsid). Of these, S, E, and M are incorporated into the virion lipidic envelope, and S protein is involved in fusion with host membranes during entry into cells. The M protein is the most abundant constituent of coronaviruses and gives the virion envelopes their shape; the E protein is only a minor constituent of the virion but is abundantly expressed inside the infected cell [88-90].

The E protein in SARS-CoV is the shortest, with only 76 amino acids, whereas that of IBV E is one of the longest (109 amino acids). E protein sequences are extremely divergent in their sequence, but the same general architecture is found in all of them: a short hydrophilic N-terminus (8–12 residues), an N-terminal TM domain (21–29 residues) followed by a cluster of 2-3 cysteines which are likely to be palmitoylated, and finally a less hydrophobic C-terminal tail (39–76 residues). Prediction of TM domains of representatives of coronavirus E pro-

teins from several species using a hidden Markov model (e.g., http://phobius.sbc.su.se/) [91] shows that they have at least one α-helical TM domain. In some cases a second TM domain is also predicted, e.g., in IBV E and MHV E (Fig 3). However, in none of these coronavirus E proteins this second putative TM has a predicted α-helical conformation. Instead, a β-coil-β motif appears to predominate in that part of the sequence, with a totally conserved Pro residue in a central position ('P' in Fig. 3).
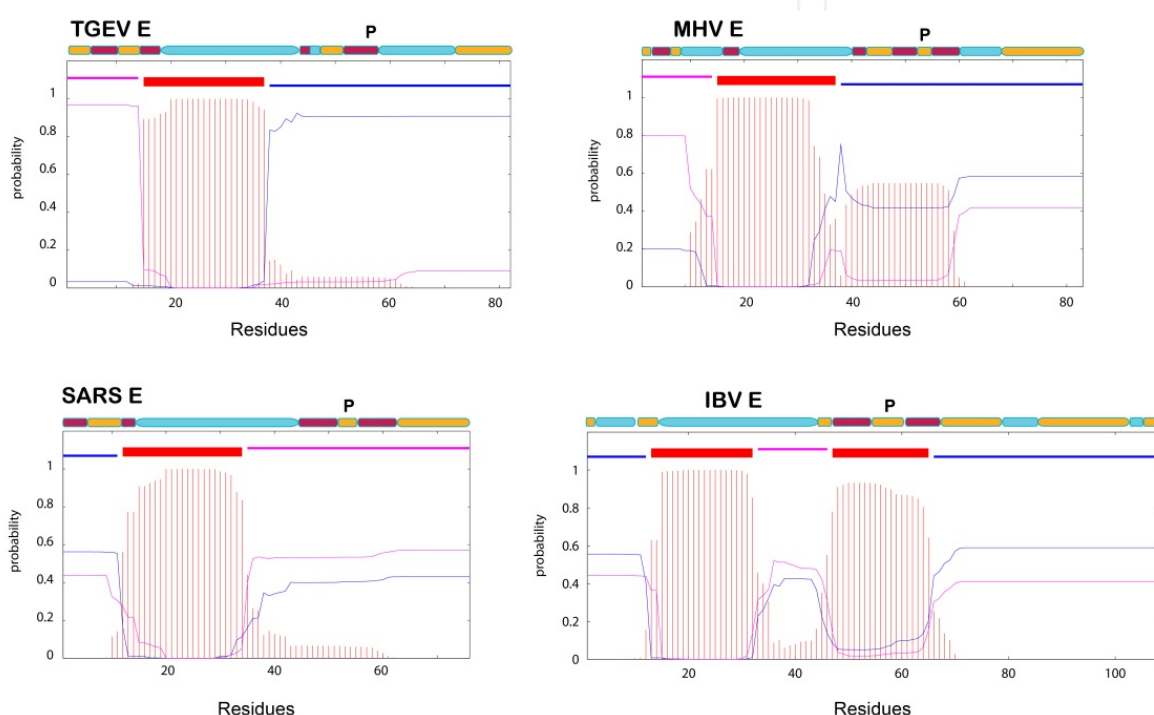

Figure 3. Secondary structure and TM prediction of E proteins of coronaviruses. E proteins from four representatives of coronavirus are presented: TGEV, MHV, SARS-CoV and IBV E proteins. Regions predicted to be α-helical, β-sheet, or random coil are marked in blue, red, and yellow, respectively. Red bars show the probability of a region being a TM domain. The location of the conserved Pro residue in each protein is indicated by a 'P'.

Topology of E proteins. The topology of coronavirus envelope proteins is an issue still under debate. Experimental determination of E protein orientation in infected cells [88, 92, 93] has shown that in TGEV E, the N-terminus is exposed to the cytoplasm, with the C-terminus facing the Golgi lumen ($N_{cyto}C_{exo}$). In MHV E, both N and C-terminal ends were found to face the cytoplasm ($N_{cyto}C_{cyto}$). For SARS-CoV E, an $N_{cyto}C_{cyto}$ topology, similar to MHV E, was reported in transfected cells [94], consistent with two TM domains ($N_{cyto}C_{cyto}$), although a small fraction of the population (~10%) was found to be glycosylated at residue N66. As glycosylation must have occurred in the Golgi lumen, the authors suggested the existence of

a minor fraction of E protein in an $N_{cyto}C_{exo}$ topology. However, a study in infected cells detected the C terminus oriented cytoplasmically and the N-terminus lumenally [95], consistent with a single TM domain. Lastly, in IBV E, the C-terminus was found exposed to the cytoplasm, but not the N-terminus, suggesting a topology $N_{exo}C_{cyto}$, with the N-terminus facing the lumen of the Golgi [96].

The results of these experiments should be interpreted with caution, especially comparing data from transfected cells and infected cells. Equally, the possible lack of accessibility to antibodies of parts of the protein plays a part. Indeed, as discussed elsewhere [97], in the case of IBV E, if the entire N-terminal region of IBV E protein was buried within the intracellular membrane, it would have remained inaccessible to the antibodies used. Several coexisting forms may exist for E proteins, which would have different roles in the life cycle of the virus.

The factors that would favour one topology over another are unknown, but one possible candidate is palmitoylation. Indeed, E proteins of SARS [26], IBV [98] and MHV [99] are palmitoylated at one or more cysteines. This modification is likely to have structural and functional consequences, because removal of the cysteines in MHV E resulted in deformed viruses [100, 101]. Experimental determination of the topology of these E protein homologs – with or without palmitoylation – in model membranes or membrane-like detergents is critical to understand the function of the envelope protein in coronavirus biology. Unfortunately, these detailed structural studies are still not available.

The importance of the correct topology in E proteins may be highlighted by a recent study [102] that showed that E protein in MHV could be replaced by some heterologous E proteins. The MHV virus became viable when the replacement was from groups 2, i.e., β-coronaviruses (SARS-CoV E) and 3, i.e., γ-coronaviruses (IBV E), but not when TGEV E (group 1, or α-coronaviruses) was used. This discrimination may have to do with topology considerations, because the contribution of E proteins to the formation of viral particles in coronaviruses could be provided by a broad range of sequences, and not by specific interactions.

Localization of E protein during viral infection. E protein can be found between the ER and Golgi compartments inside the cell [103-105]. However, only a small amount ends up in the virion [88-90], suggesting that its main role is inside the cell [95]. In transfected HeLa cells, SARS-CoV E protein is targeted to the Golgi complex, and this localization has been attributed, at least in part, to the β-hairpin motif in its C-terminus [106] (see Fig. 3). In infected Vero E6 cells, SARS-CoV E protein accumulates in the ER-Golgi intermediate compartment (ERGIC) [95]; the latter study could not detect any SARS-CoV E protein in the plasma membrane.

Effect of coronavirus E gene deletion. While the absence of S and M protein are clearly deleterious to the virus because of their abundance and key role in envelope formation, the E protein is not essential for *in vitro* or *in vivo* coronavirus replication. However, the absence of E protein results in an attenuated virus, as shown for SARS-CoV [107] and other coronaviruses (see below). Recently, it has been shown that SARS viruses lacking gene E, in addition to being attenuated, did not grow in the central nervous system, in contrast to the wild type

virus [108]. This suggests a role of the SARS-CoV E gene as a virulence factor influencing tissue tropism and pathogenicity. Recently, SARS-CoV lacking E gene has been suggested as vaccine candidate [109]. Studies using the E deleted SARS-CoV E have shown that E protein affects stress and inflammation responses [110], which probably contribute to the attenuation of the virus observed in the absence of this protein [107].

In other coronaviruses, it has been found that E protein is involved in viral morphogenesis, e.g., co-expression of M and E is sufficient for formation and release of virus-like particles (VLP) in the host cell [93, 111-115]. Also, mutations in the extramembrane domain of E protein were shown to impair viral assembly and maturation in MHV [116], probably due to a defective interaction with M protein. In TGEV, the absence of E protein resulted in a blockade of virus trafficking in the secretory pathway, and the prevention of virus maturation [117, 118].

Interaction partners of E proteins. The interaction of E protein with M in IBV has already been reported by two different labs [96, 119] and involves at least the C-terminal tail of these two proteins, which therefore should be on the same side of the lipid bilayer. Additionally, the extramembrane cytoplasmic tail of SARS-CoV E has also been reported to bind Bcl-X_L [120] and the N-terminal domain of non-structural protein 3 (nsp3) [121]. Similar studies have shown that SARS-CoV E via its four last C-terminal amino-acids, interacts with the host protein, PALS1, a tight junction-associated protein. Intercellular tight junctions are a physical barrier that protects underlying tissues from pathogen invasions. In SARS-CoV–infected Vero E6 cells, PALS1 redistributes to the ERGIC/Golgi region, where E accumulates. Hijacking PALS1 by SARS-CoV E may play a determinant role in the disruption of the lung epithelium in SARS patients [122]. SARS-CoV E has also been found to interact with Na^+/K^+ ATPase α-1 subunit and stomatin [95].

Channel activity in coronavirus E proteins. Enhanced permeability has been observed in bacterial and mammalian cells expressing MHV E [123] or SARS-CoV E [26]. In addition, E proteins of SARS, human coronavirus 229E, MHV, and IBV, have shown *in vitro* ion channel activity in planar lipid bilayers [124, 125], which in some cases was inhibited by the drug hexamethylene amiloride (HMA) [125]. In a patch clamp study, channel activity was observed in cells transfected with SARS-CoV E [25], although another study could not detect SARS-CoV E protein in the plasma membrane of transfected or infected cells [95]. Nevertheless, channel activity has been shown in black lipid membranes for purified synthetic TM domains and full length SARS-CoV [67, 126, 127], and inactivating mutations located in the TM domain, N15A and V25F [126], have been confirmed recently in a separate study [128]. In the latter, a significant contribution of lipid composition was observed, and a protein-lipid complex forming pore was proposed. These mutants may help elucidate the contribution of channel activity to SARS-CoV E protein function.

Structural determination of E protein. At present, detailed structures of coronavirus envelope proteins are lacking. This is due difficulties in both expression and purification, and to their high tendency to aggregate which makes crystallization and NMR studies extremely challenging. Recently, we have successfully utilized a modified β-barrel fusion protein construct to express and subsequently purify full-length SARS-CoV E and IBV E proteins [67].

We showed that both full length proteins form homopentamers, confirming previous results obtained only with the synthetic TM domain [25].

Previous reports have studied the oligomerization of coronavirus E proteins. However, results were not conclusive, partly because these experiments were performed in SDS, a harsh detergent that leads to monomers or to non-specific aggregates. For example, SARS-CoV E oligomerization has been studied in Western Blots after SDS-PAGE and labeling with polyclonal antibodies [99], antibodies against a hemagglutinin-derived C-terminal tag [100], or using non purified or truncated synthetic E proteins [124, 125]. In the latter approach, a predominanly monomeric form was observed in SDS. In our hands, synthetic SARS-CoV E also produced in SDS mostly monomers, and a minor fraction of dimers (unpublished observations), but several oligomers were observed for the recombinant form (Fig. 4, lane WT). The differences between synthetic and recombinant E protein may be due to unwanted side reactions that take place during synthesis. Addition of DTT (Fig. 4B) produces bands compatible with monomers and trimers, whereas cysteine-less mutants only produced monomers. Thus, the three cysteines in SARS-CoV E seem to participate in some inter-monomeric contacts. Indeed, sedimentation data for SARS-CoV E could only be fitted after addition of reductant [67] in the case of SARS-CoV E. Differences between absence and presence of reductant were observed even when only one cysteine was available (Fig. 4B), therefore these disulfide bonds may not be specific. Changes in hydrophobicity and local secondary structure seem to play a major role in the results observed. Further, disulfide bonds are not necessary to form pentamers; sedimentation equilibrium of full-length SARS-CoV E or IBV E in C14SB detergent and in the presence of reducing agent produced best fit to a monomer-pentamer equilibrium model [67], similar to what has been observed for the TM region alone [127].

The likely orientation of these cysteine residues relative the pentameric bundle can be determined on the basis of the available structure formed by synthetic TM_{8-38} [25]. That structure did not include any of the three cysteines of SARS-CoV E, but if the structural model is prolonged by two turns (Fig. 5), the three cysteines are seen oriented either towards the lumen of the channel or inter-helically.

The juxtamembrane cysteines in coronavirus envelope proteins are well conserved, and have been found to be crucial in the coronavirus cycle. For example, in MHV E, removal of the cysteines resulted in deformed viruses [99-101]. Using the full length infectious clone [99], double- and triple-mutants to alanine produced smaller plaques and decreased virus yields. Single-substitution mutants, in contrast, did not produce anomalous growth, whereas replacement of all three cysteines resulted in crippled virus with significantly reduced yields. In these reports, these effects were attributed to the absence of palmitoylation sites, which may direct E proteins towards lipid rafts [129]. E proteins of SARS [26], IBV [98] and MHV [99] have been shown to be palmitoylated at one or more cysteines. It is possible that an additional role of palmitoylation is to drag the C-terminal tail of E proteins towards the membrane and trigger a conformational change.
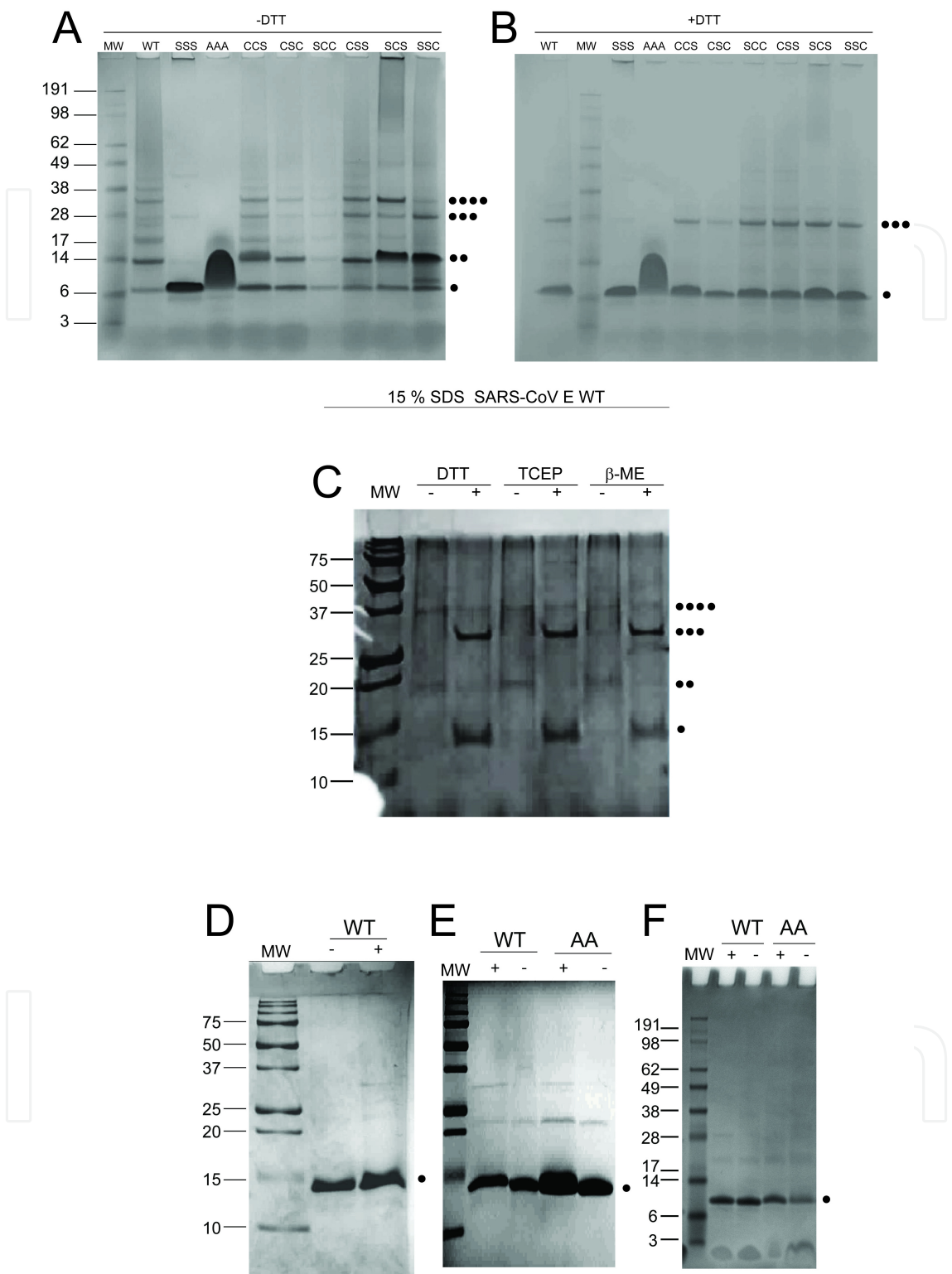
Figure 4. SDS-PAGE electrophoresis of SARS-CoV E and IBV E. (A) SARS-CoV E wild type (WT) and cysteine mutants in the absence of DTT in gel 4-12 % Nu-PAGE in MES/SDS buffer; (B) same as A in presence of DTT. The lane containing the molecular weight markers (MW) is indicated. The oligomeric size is indicated by black circles (●); (C) Effect of three reductants (DTT, TCEP and β-mercaptoethanol (β-ME) on the electrophoretic mobility SARS-CoV E WT in 15% SDS PAGE gel.
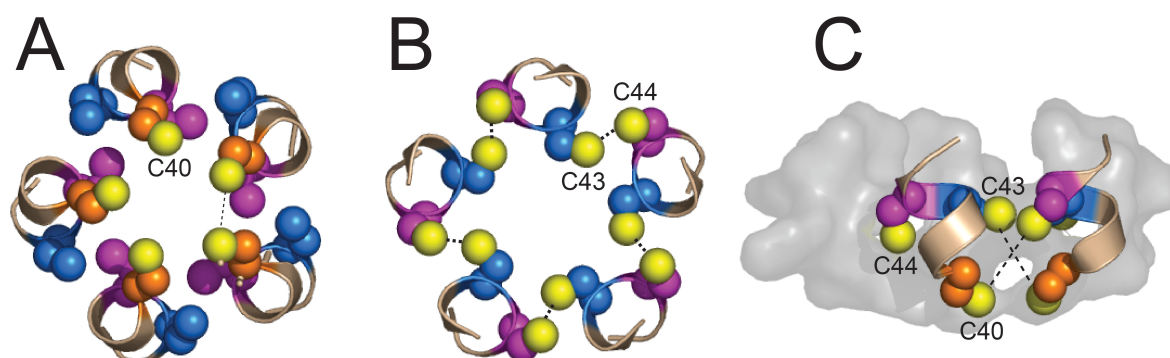
Figure 5. Cysteine location in the pentameric arrangement of the TM domain of SARS-CoV E. The scheme is arranged according to previous published models [25, 130] after prolonging the helices 2 turns at the C-terminal end, and shows the position of the three cysteines in SARS-CoV E, C40, C43 and C44; A and B, views from the N-terminus of the pentamer, with C40 (A) and C43 and C44 (B); C, Side view, showing only two helices for clarity, and possible interhelical disulfide bonds C43-C40 and C44-C40.

Dissection of the domains of SARS-CoV E. The four representatives of CoV E proteins have a predicted α-helical TM domain (Fig. 6a) and a C-terminal region predicted to have β-structure. Synthetic peptide 36-76 encompasses the C-terminal extramembrane domain and was analyzed in the presence of DMPC lipid membranes using FTIR. This peptide presented limited solubility both in water and in organic solvents. The amide I spectrum of this peptide (Fig. 6b) shows bands assigned to antiparallel β-sheet, because of the splitting of the amide I band caused by strong inter- and intra-strand transition dipole coupling (TDC) [131-133], resulting in a weak band at high frequency (1675–1690 cm^{-1}) and a strong band at lower frequency (1625–1640 cm^{-1}). The band at 1666 cm^{-1} can be assigned to disordered structure [134, 135]. The amide A frequency was blue-shifted from that observed for the TM domain alone [130] (3,305 cm^{-1}) or full length SARS-CoV E (3294 cm^{-1}, not shown) to 3281 cm^{-1}, again consistent with the presence of β-structure. The intensity of the amide II band decreased upon exposure to D$_2$O (dotted line, Fig. 6b) by about 30 ± 5%, i.e., ~28 residues are resistant to exchange in this peptide. The fast-exchanging fraction is likely due to the region predicted to have random coil conformation. Thus, the 36-76 fragment has an intrinsic tendency to fold as β-sheet, and presents both β-structure and random coil, in agreement with the secondary structure prediction (Fig. 6a). In fact, the spectrum resulting from the addition of TM α-helix (8-38) [130] and C-terminal tail (36-76), shown in Fig. 6b, is very similar to the

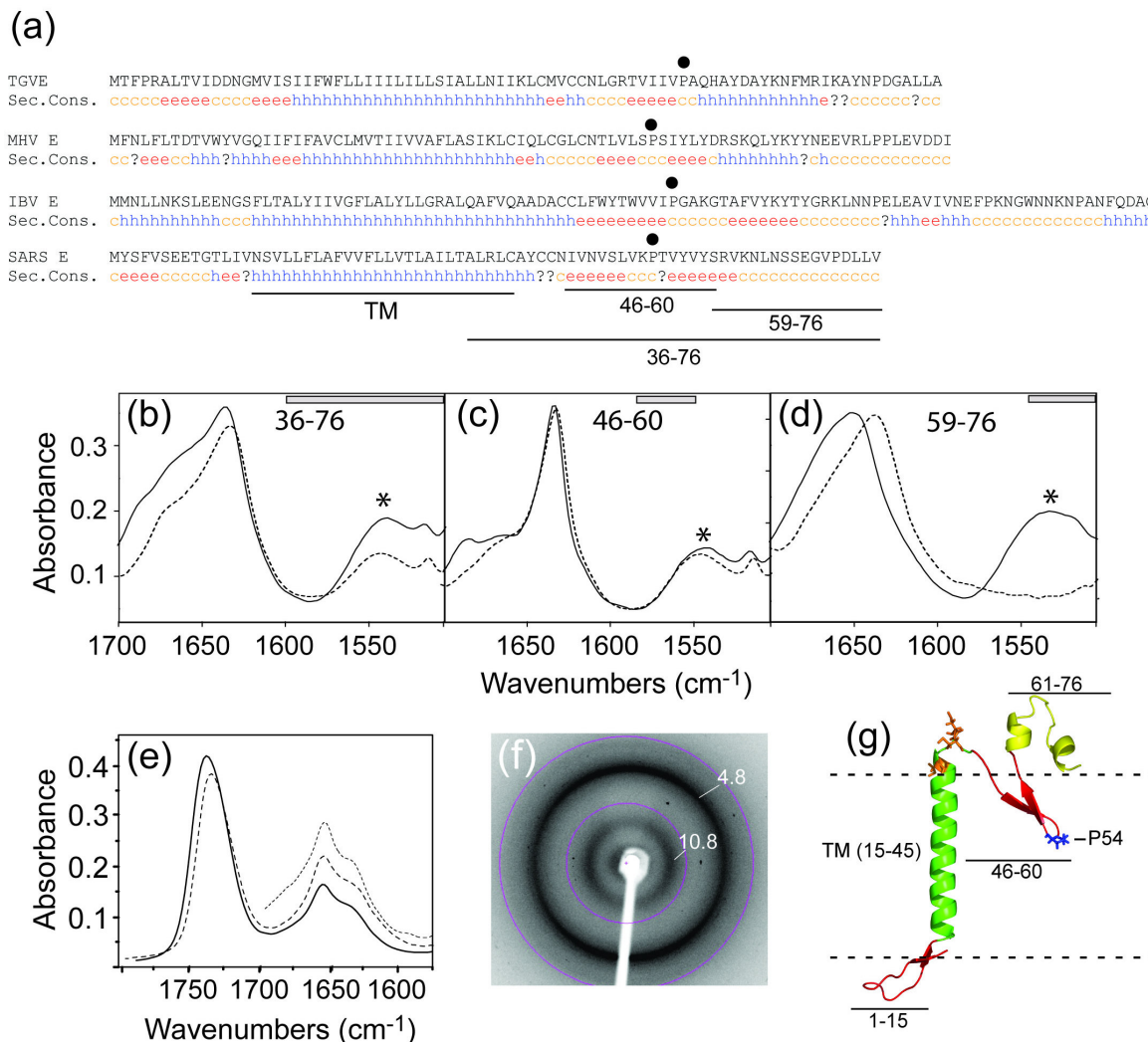spectrum obtained for full length SARS-CoV E (Fig. 6e, dotted line) reconstituted in the same conditions.

Figure 6. Secondary structure prediction of coronavirus envelope proteins and correspondence with results obtained for synthetic peptides of SARS-CoV E. (a) Sequences corresponding to E proteins representative of coronavirus groups 1 (TGEV E), 2 (MHV E), 3 (IBV E) and SARS CoV E, and their predicted secondary structure (consensus)[136]. The position of the conserved proline is indicated with a black dot; (b-d) amide I and II bands of the synthetic SARS-CoV E peptides indicated when incorporated in DMPC bilayers in H_2O (solid) or after D_2O (dash) hydration. The position of amide II band is indicated by a star; (e) ATR-FTIR spectra corresponding to SARS-CoV E (solid line), and IBV E (broken line) reconstituted in DMPC bilayers, in the lipid ester region (1740 cm⁻¹) and amide I region (C=O stretching, 1650 cm⁻¹). The dotted line resulted from the addition of the spectra corresponding to the TM [130] and fragment 36-76 (panel b); (f) X-ray diffraction pattern for peptides (36-76) or (46-60) after drying from acetonitrile. The inter-sheet spacing is 10.8 Å (inner ring) whereas the hydrogen bond spacing is represented by the outer ring at 4.8 Å, characteristic of amyloid fibrils. Due to poor alignment, the reflection at distance 4.8 Å appeared as a ring; (g) schematic model of full length SARS-CoV E build using prediction tools and experimental data obtained using infrared spectroscopy.

Similar experiments with fragments 46-60 and 59-76 (Fig. 6, c-d) showed that 46-60 forms β-sheets resistant to H/D exchange. Indeed, this latter peptide showed limited solubility, similar to the 'parent' peptide 36-76. Further, its amide I spectrum in DMPC displayed the

features of antiparallel β-sheet, with bands at 1635 cm^{-1} and 1685 cm^{-1} (Fig. 6c) and showed no H/D exchange in the amide II region (Fig. 6c, star). In contrast, fragment 61-76 is predicted to form random coil (Fig. 6a), and should show complete H/D exchange. Indeed, the hydrophilic fragment 59–76 dissolved readily in water (>5 mg/ml), produced an amide I spectrum in DMPC consistent with random structure (Fig. 6d), with a broad amide I band at 1645 cm^{-1}, and showed complete H/D exchange at the amide II region (star).

The two folding domains observed in the C-terminal domain of SARS-CoV E are reminiscent of the two separate domains reported for the amyloid peptide [137], where fragment 34–42 has limited solubility and adopts antiparallel β-sheet structure, and fragment 26–33 is more soluble in water, and has a disordered conformation. Thus, we tested if peptide (36-76) can form amyloid-like fibrils. The aggregate obtained after drying this peptide from acetonitrile showed intense X-ray reflections at ~4.8 Å and ~10.8 Å (Fig. 6f), which correspond to the distances between hydrogen bonded peptide backbones and β–pleated sheets, respectively, characteristically found in Alzheimer disease amyloid plaque cores [137]. This peptide was monomeric in SDS. Based on the above results, a topological model for SARS-CoV E can be proposed, with one α-helical TM domain and a C-terminal β-hairpin (Fig. 6g). We have reported previously that SARS-CoV E secondary structure in lipid bilayers is predominantly α-helical [67], in contrast with the results shown in Fig. 6e. However, we have found that the secondary structure of E protein is strongly dependent on the reconstitution conditions. In our previous report [67], the protein was presolubilized in hexafluoroisopropanol, an α-helix inducer, whereas in Fig. 6e pre-solubilization was done in methanol. Thus, the β-hairpin prediction for the residues around the highly conserved residue P54, may be correct only in certain experimental conditions. The dual conformation, α-helical and β-hairpin, conformation proposed here is reminiscent of the proposed dual topology of a similar β-hairpin with central conserved Pro residue found in stomatin. In that case, secondary structure changed to α-helix when Pro was mutated to Ser [138].

Examination of the peptide (36-76) precipitate by electron microscopy (Fig. 7A) revealed a protofibrillar morphology [139-141]. These structures were not observed in the control specimen prepared in the absence of peptide (Fig. 7B). The fibrils form an ordered mesh structure characterized by straight sections intervened by bends. The fibril width was 7, 8 and 10 nm, consistent with reports of other filaments derived from β-sheet structures [141-143]. The length of the straight sections was rather homogenous, with most measurements falling between 20-40 nm and with an average value of 32 nm.

The formation of fibrils is anticipated by the residue composition in the region around the conserved proline (P54). For example, from the 17 residues in the stretch I46 to V62, 9 residues are either V, I or Y. Amino acids with β-branched side chains, e.g. valine and isoleucine, or bulky residues, have been shown previously to disfavor α-helical conformation, and to pack efficiently along the surface of a β-sheet [144, 145]. Accordingly, a series of hexapeptides containing similar motifs (e.g., VxVx) have been shown to be good amyloid-forming peptides [146]. We speculate that changing some of these residues to non-branched, for example from V to L, would abolish the ability of SARS-CoV E to form fibers, and possibly

attenuate the observed cytopathological effects of SARS-CoV E in cells. Indeed, a similar strategy led to disruption of Golgi targeting in SARS-CoV E [106].
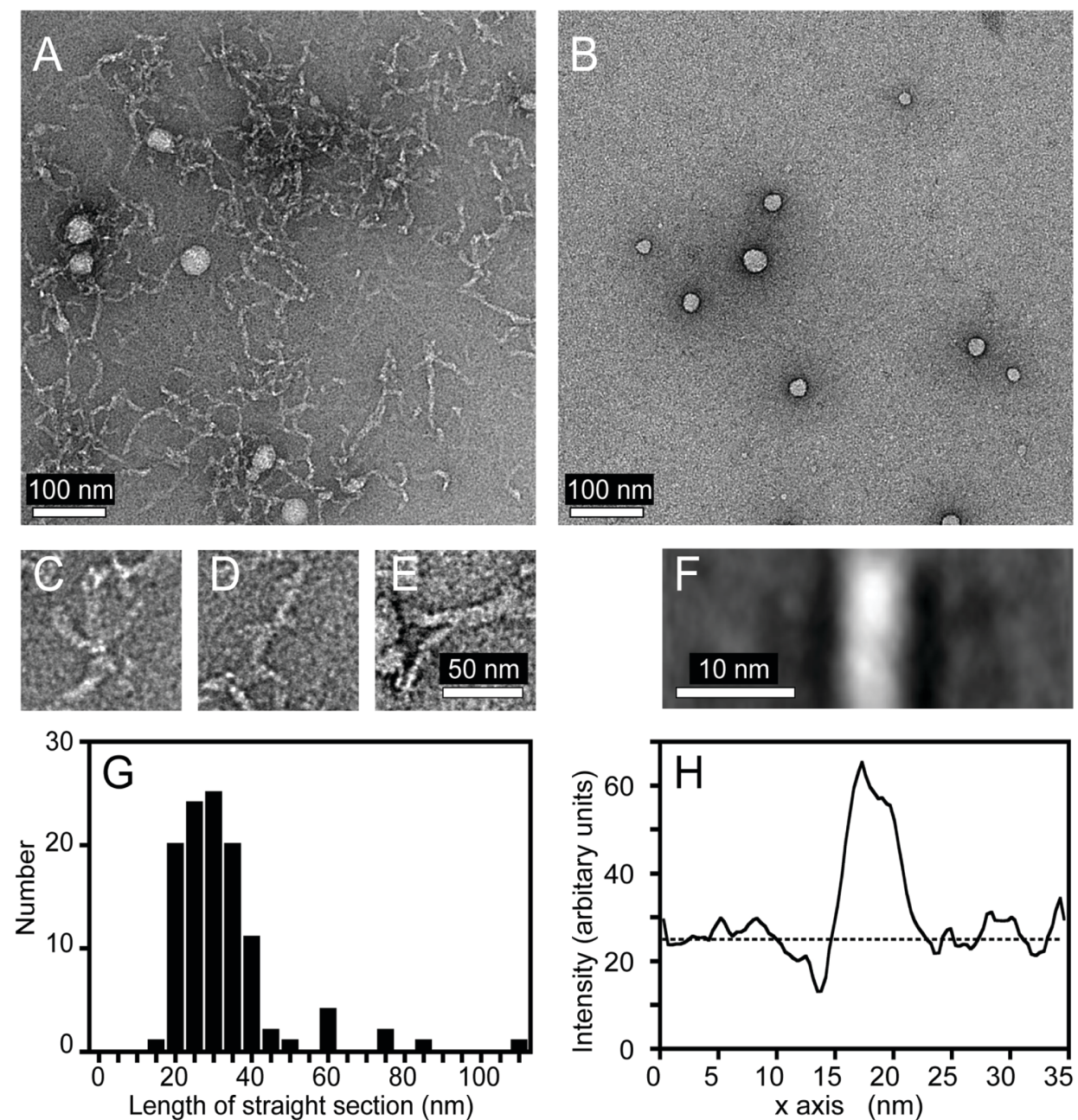

Figure 7. Electron microscopy and image processing; (A) Micrograph of a negatively stained sample of peptide 36-76 dissolved in acetonitrile. The ordered mesh is formed by 7-10 nm wide fibrils with 20-40 nm long straight sections. Globular structures of 10-50 nm diameter are also present; (B) Control specimen without peptide showing similar globular structures; (C, D) Magnified views of fibril branching points; (E) Two thin fibrils merging into a thicker one; (F) Class average of the 8 nm fibril; (G) Histogram of the lengths of the fibril straight sections. (H) Intensity profile along the x-axis of panel (F). The width of the peak above background level indicates filament thickness. The scale bar is shown in each panel.

In addition, a sequence of ordered fragments (α-helices or strands) flanking a disordered or turn loop, with Pro at its center, has been described for several fusion peptides, e.g., in EnvA of the Avian sarcoma/leukosis virus subtype A (ASLV-A) [147], Ebola virus GP [148] and mouse or macaque fertilin α (ADAM 1) [149], which suggests that this part of SARS-CoV E is analogous to an internal fusion peptide. This motif has also been observed in a cis-proline turn [150] linking two β-hairpin strands in the structure of an HIV-1$_{III}$B V3 peptide. It was found by mutagenesis of the fusion peptide of Env in ASLV-A, that proline, or a residue of similar intermediate hydrophobicity, are part of an accessible loop and was needed for initial interactions of fusion peptides with target membranes.

Amyloid fiber formation has been reported for fragments of many non pathogenic proteins [151], and they have been found in a variety of proteins which are not associated with disease [152, 153]. Therefore, this finding may not have relevance for the toxicity of the virus. Nevertheless, this possibility cannot be discarded in view of other roles of similar semen-derived fibers in HIV viral entry which dramatically enhance HIV infection [154]. A more likely possibility, however, is that this conformational plasticity is needed during membrane fusion; a transition form a α-helical conformation to an antiparallel β-structure, with Pro as a hinge, could drive membrane fusion by pulling the two membranes in close apposition.

NMR studies: towards the high-resolution structure of SARS-CoV E. Full-length SARS-CoV E protein shows a high tendency to aggregate when solubilized in detergents, making it difficult to find a suitable condition for structural determination. While the TM region could be studied in DPC [25], 2D-HSQC spectra of full-length SARS-CoV E protein show poor quality in DPC-solubilized samples, even when SDS is included to improve spectral quality (Fig. 8A). Some degree of improvement can be observed with a truncated version of SARS-CoV E, which is lacking ~10 amino acids at both termini (Fig. 8B). We have also obtained a good, well-dispersed spectrum for this construct in SDS (Fig. 8C), allowing us to begin the structural determination of the extramembrane regions of SARS-CoV E.
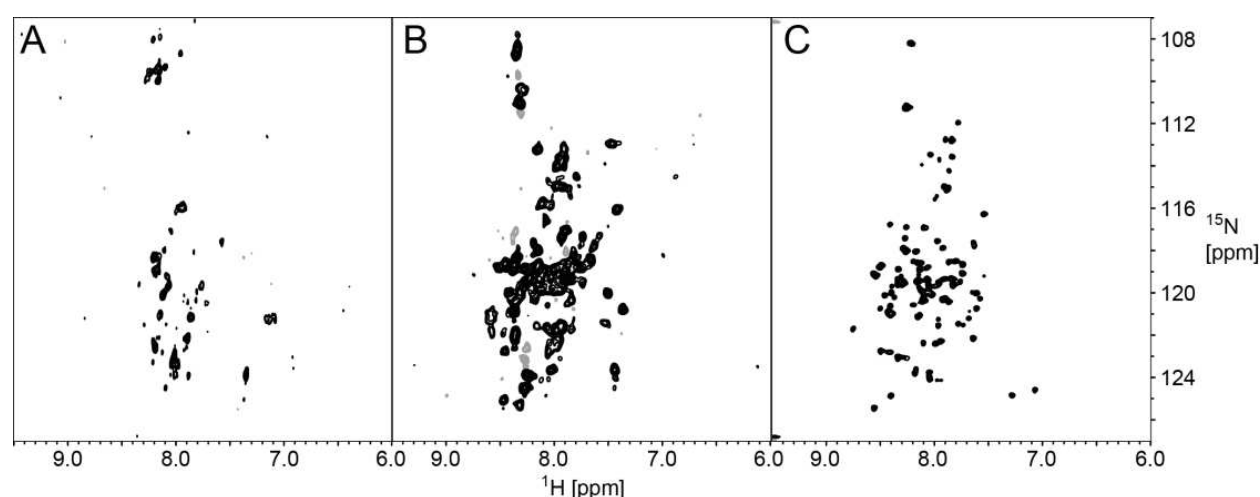

Figure 8. TROSY-HSQC of SARS-CoV E protein in various detergent micelles. (A) full-length SARS-CoV E in a mixture of DPC and SDS, (B) truncated SARS-CoV E in DPC and (C) in SDS.

3. Conclusion

Viroporins constitute important components of viruses, and we are just beginning to understand what is their biological role during the viral life cycle. One of the main problems in their *in vitro* structural and functional study is high hydrophobicity and strong tendency to aggregate. This may reflect their likely multifunctional role in the cell, interacting with several viral and host partners. This multifunctionality seems dictated by genetic minimalism observed in viruses, in turn forced by the need to rapidly produce new progeny inside an alien environment. Viroporins such as those presented here, SH protein and CoV E proteins, form complexes that are still not well characterized that are critical for viral eggress. In this context, the biological function of channel activity is still unknown. More data is becoming available with more purified proteins, and inevitably extrapolations will have to be made from easier to handle proteins. For example, we could obtain a reasonably detailed SH protein NMR spectrum in detergents, but that is still not possible for E proteins. Even when structural data can be obtained, efforts will be directed towards environments that best mimic the conditions of natural lipid bilayers, as protein conformation is likely to change. With multidisciplinary action, the key roles of viroporins will be elucidated in the near future.

Acknowledgements

Author details

Wahyu Surya[1], Montserrat Samsó[2] and Jaume Torres[1*]

*Address all correspondence to: jtorres@ntu.edu.sg

1 School of Biological Sciences, Nanyang Technological University, Singapore

2 School of Medicine, Virginia Commonwealth University, Richmond, VA, USA

References

[1] Gonzalez, M.E. and L. Carrasco, Viroporins. FEBS Lett., 2003. 552(1): p. 28-34.

[2] Carrasco, L., *Membrane leakiness after viral infection and a new approach to the development of antiviral agents.* Nature, 1978. 272(5655): p. 694-699.

[3] Carrasco, L., *Modification of Membrane Permeability by Animal Viruses*, in *Advances in Virus Research*, F.A.M. Karl Maramorosch and J.S. Aaron, Editors. 1995, Academic Press. p. 61-112.

[4] Bukreyev, A., et al., *Recombinant respiratory syncytial virus from which the entire SH gene has been deleted grows efficiently in cell culture and exhibits site-specific attenuation in the respiratory tract of the mouse.* J Virol, 1997. 71(12): p. 8973-82.

[5] Whitehead, S.S., et al., *Recombinant respiratory syncytial virus bearing a deletion of either the xlink or SH gene is attenuated in chimpanzees.* J Virol, 1999. 73(4): p. 3438-42.

[6] Sanderson, C.M., et al., *Overexpression of the vaccinia virus A38L integral membrane protein promotes Ca2+ influx into infected cells.* J. Virol., 1996. 70(2): p. 905-914.

[7] Bour, S. and K. Strebel, *The human immunodeficiency virus (HIV) type 2 envelope protein is a functional complement to HIV type 1 Vpu that enhances particle release of heterologous retroviruses.* J. Virol., 1996. 70(12): p. 8285-8300.

[8] Shai, Y., *Mechanism of the binding, insertion and destabilization of phospholipid bilayer membranes by alpha-helical antimicrobial and cell non-selective membrane-lytic peptides.* Biochim. Biophys. Acta - Biomem., 1999. 1462(1-2): p. 55-70.

[9] Shimbo, K., et al., *Viral and cellular small integral membrane proteins can modify ion channels endogenous to Xenopus oocytes.* Biophys. J., 1995. 69(5): p. 1819-29.

[10] Hsu, K., et al., *Mutual functional destruction of HIV-1 Vpu and host TASK-1 channel.* Mol. Cell, 2004. 14(2): p. 259-267.

[11] Song, W.F., et al., *Respiratory Syncytial Virus Inhibits Lung Epithelial Na(+) Channels by Up-regulating Inducible Nitric-oxide Synthase.* J. Biol. Chem., 2009. 284(11): p. 7294-7306.

[12] Lazrak, A., et al., *Influenza virus M2 protein inhibits epithelial sodium channels by increasing reactive oxygen species.* FASEB J., 2009. 23(11): p. 3829-3842.

[13] Cuconati, A., et al., *A protein linkage map of the P2 nonstructural proteins of poliovirus.* J. Virol., 1998. 72(2): p. 1297-1307.

[14] Strauss, J.H. and E.G. Strauss, *The alphaviruses: Gene expression, replication, and evolution.* Microbiological Reviews, 1994. 58(3): p. 491-562.

[15] Sanz, M.A., L. Peìrez, and L. Carrasco, *Semliki forest virus 6K protein modifies membrane permeability after inducible expression in Escherichia coli cells.* J. Biol. Chem., 1994. 269(16): p. 12106-12110.

[16] Melton, J.V., et al., *Alphavirus 6K proteins form ion channels.* J. Biol. Chem., 2002. 277(49): p. 46923-31.

[17] Schubert, U., et al., *Identification of an ion channel activity of the Vpu transmembrane domain and its involvement in the regulation of virus release from HIV-1-infected cells.* FEBS Lett., 1996. 398(1): p. 12-18.

[18] Chen, M.Y., et al., *Human immunodeficiency virus type 1 Vpu protein induces degradation of CD4 in vitro: The cytoplasmic domain of CD4 contributes to Vpu sensitivity.* J. Virol., 1993. 67(7): p. 3877-3884.

[19] Lamb, R.A., L.J. Holsinger, and L.H. Pinto, *The influenza A virus M2 ion channel protein and its role in the influenza virus life cycle.* Receptor-Mediated Virus Entry into Cells, 1994: p. 303-321.

[20] Perez, M., et al., *Membrane permeability changes induced in Escherichia coli by the SH protein of human respiratory syncytial virus.* Virology, 1997. 235(2): p. 342-51.

[21] Bodelon, G., et al., *Modification of late membrane permeability in avian reovirus-infected cells: viroporin activity of the S1-encoded nonstructural p10 protein.* J. Biol. Chem., 2002. 277(20): p. 17789-96.

[22] Penin, F., et al., *Structural biology of hepatitis C virus.* Hepatology (Baltimore, Md, 2004. 39(1): p. 5-19.

[23] Harada, T., N. Tautz, and H.J. Thiel, *E2-p7 region of the bovine viral diarrhea virus polyprotein: Processing and functional studies.* J. Virol., 2000. 74(20): p. 9498-9506.

[24] Plugge, B., et al., *A potassium channel protein encoded by chlorella virus PBCV-1.* Science, 2000. 287(5458): p. 1641-1644.

[25] Pervushin, K., et al., *Structure and inhibition of the SARS coronavirus envelope protein ion channel.* PLoS Path., 2009. 5(7).

[26] Liao, Y., et al., *Biochemical and functional characterization of the membrane association and membrane permeabilizing activity of the severe acute respiratory syndrome coronavirus envelope protein.* Virology, 2006. 349(2): p. 264-275.

[27] Nieva, J.L., V. Madan, and L. Carrasco, *Viroporins: structure and biological functions.* Nature Reviews Microbiology, 2012. 10(8): p. 563-574.

[28] Wang, K., S. Xie, and B. Sun, *Viral proteins function as ion channels.* Biochim. Biophys. Acta, 2011. 1808(2): p. 510-5.

[29] Grambas, S. and A.J. Hay, *Maturation of Influenza-a Virus Hemagglutinin - Estimates of the Ph Encountered during Transport and Its Regulation by the M2 Protein.* Virology, 1992. 190(1): p. 11-18.

[30] Sakaguchi, T., G.P. Leser, and R.A. Lamb, *The ion channel activity of the influenza virus M2 protein affects transport through the Golgi apparatus.* J. Cell Biol., 1996. 133(4): p. 733-747.

[31] Stouffer, A.L., et al., *Structural basis for the function and inhibition of an influenza virus proton channel.* Nature, 2008. 451(7178): p. 596-9.

[32] Schnell, J.R. and J.J. Chou, *Structure and mechanism of the M2 proton channel of influenza A virus.* Nature, 2008. 451(7178): p. 591-5.

[33] Pielak, R.M., J.R. Schnell, and J.J. Chou, *Mechanism of drug inhibition and drug resistance of influenza A M2 channel.* Proc. Nat. Acad. Sci. USA, 2009. 106(18): p. 7379-7384.

[34] Cady, S.D., T.V. Mishanina, and M. Hong, *Structure of Amantadine-Bound M2 Transmembrane Peptide of Influenza A in Lipid Bilayers from Magic-Angle-Spinning Solid-State NMR: The Role of Ser31 in Amantadine Binding.* J. Mol. Biol., 2009. 385(4): p. 1127-1141.

[35] Wang, J., et al., *Discovery of spiro-piperidine inhibitors and their modulation of the dynamics of the M2 proton channel from influenza A virus.* J. Am. Chem. Soc., 2009. 131(23): p. 8066-8076.

[36] Skehel, J.J., A.J. Hay, and J.A. Armstrong, *On the mechanism of inhibition of influenza virus replication by amantadine hydrochloride.* J Gen Virol, 1978. 38(1): p. 97-110.

[37] Dowell, S.F., et al., *Respiratory syncytial virus is an important cause of community-acquired lower respiratory infection among hospitalized adults.* J Infect Dis, 1996. 174(3): p. 456-62.

[38] Delgado, M.F., et al., *Lack of antibody affinity maturation due to poor Toll-like receptor stimulation leads to enhanced respiratory syncytial virus disease.* Nat. Med., 2009. 15(1): p. 34-41.

[39] Collins, P.L. and J.A. Melero, *Progress in understanding and controlling respiratory syncytial virus: Still crazy after all these years.* Virus Res., 2011. 162(1-2): p. 80-99.

[40] Melero, J.A., *Molecular Biology of Human Respiratory Syncytial Virus*, in *Respiratory Syncytial Virus*, P. Cane, Editor 2007, Elsevier B.V. p. 1-41.

[41] Krusat, T. and H.J. Streckert, *Heparin-dependent attachment of respiratory syncytial virus (RSV) to host cells.* Arch Virol, 1997. 142(6): p. 1247-54.

[42] Lamb, R.A., *Paramyxovirus fusion: a hypothesis for changes.* Virology, 1993. 197(1): p. 1-11.

[43] Fields, B.N., D.M. Knipe, and P.M. Howley, Fields Virology, 1996.

[44] Roberts, S.R., R.W. Compans, and G.W. Wertz, *Respiratory syncytial virus matures at the apical surfaces of polarized epithelial cells.* J. Virol., 1995. 69(4): p. 2667-2673.

[45] Lindquist, M.E., et al., *Respiratory syncytial virus induces host RNA stress granules to facilitate viral replication.* J. Virol., 2010. 84(23): p. 12274-12284.

[46] Brock, S.C., et al., *The transmembrane domain of the respiratory syncytial virus F protein is an orientation-independent apical plasma membrane sorting sequence.* J. Virol., 2005. 79(19): p. 12528-12535.

[47] Utley, T.J., et al., *Respiratory syncytial virus uses a Vps4-independent budding mechanism controlled by Rab11-FIP2.* Proceedings of the National Academy of Sciences of the United States of America, 2008. 105(29): p. 10209-10214.

[48] Collins, P.L. and G. Mottet, *Membrane orientation and oligomerization of the small hydrophobic protein of human respiratory syncytial virus.* J Gen Virol, 1993. 74: p. 1445-1450.

[49] Chen, M.D., et al., *Conservation of the respiratory syncytial virus SH gene.* J Infect Dis, 2000. 182(4): p. 1228-33.

[50] Collins, P.L., R.A. Olmsted, and P.R. Johnson, *The small hydrophobic protein of human respiratory syncytial virus: comparison between antigenic subgroups A and B.* J Gen Virol, 1990. 71 (Pt 7): p. 1571-6.

[51] Techaarpornkul, S., N. Barretto, and M.E. Peeples, *Functional analysis of recombinant respiratory syncytial virus deletion mutants lacking the small hydrophobic and/or attachment glycoprotein gene.* J. Virol., 2001. 75(15): p. 6825-34.

[52] Bukreyev, A., et al., *Recombinant respiratory syncytial virus from which the entire SH gene has been deleted grows efficiently in cell culture and exhibits site-specific attenuation in the respiratory tract of the mouse.* J. Virol., 1997. 71(12): p. 8973-82.

[53] Karron, R.A., et al., *Respiratory syncytial virus (RSV) SH and G proteins are not essential for viral replication in vitro: clinical evaluation and molecular characterization of a cold-passaged, attenuated RSV subgroup B mutant.* Proc. Nat. Acad. Sci. USA, 1997. 94(25): p. 13961-6.

[54] Heminway, B.R., et al., *Analysis of respiratory syncytial virus F, G, and SH proteins in cell fusion.* Virology, 1994. 200(2): p. 801-5.

[55] Techaarpornkul, S., N. Barretto, and M.E. Peeples, *Functional analysis of recombinant respiratory syncytial virus deletion mutants lacking the small hydrophobic and/or attachment glycoprotein gene.* J Virol, 2001. 75(15): p. 6825-34.

[56] Fuentes, S., et al., *Function of the respiratory syncytial virus small hydrophobic protein.* Journal of Virology, 2007. 81(15): p. 8361-6.

[57] Feldman, S.A., et al., *Human respiratory syncytial virus surface glycoproteins F, G and SH form an oligomeric complex.* Arch Virol, 2001. 146(12): p. 2369-83.

[58] Low, K.W., et al., *The RSV F and G glycoproteins interact to form a complex on the surface of infected cells.* Biochem Biophys Res Commun, 2008. 366(2): p. 308-13.

[59] Calder, L.J., et al., *Electron microscopy of the human respiratory syncytial virus fusion protein and complexes that it forms with monoclonal antibodies.* Virology, 2000. 271(1): p. 122-31.

[60] Escribano-Romero, E., et al., *The soluble form of human respiratory syncytial virus attachment protein differs from the membrane-bound form in its oligomeric state but is still capable of binding to cell surface proteoglycans.* J Virol, 2004. 78(7): p. 3524-32.

[61] Rixon, H.W.M., et al., *The respiratory syncytial virus small hydrophobic protein is phosphorylated via a mitogen-activated protein kinase p38-dependent tyrosine kinase activity during virus infection.* J Gen Virol, 2005. 86(2): p. 375-384.

[62] Gan, S.W., et al., *Structure and ion channel activity of the human respiratory syncytial virus (hRSV) small hydrophobic protein transmembrane domain.* Protein Sci, 2008. 17(5): p. 813-20.

[63] Lin, Y., et al., *Induction of apoptosis by paramyxovirus simian virus 5 lacking a small hydrophobic gene.* J Virol, 2003. 77(6): p. 3371-83.

[64] Rixon, H.W., et al., *The small hydrophobic (SH) protein accumulates within lipid-raft structures of the Golgi complex during respiratory syncytial virus infection.* J Gen Virol, 2004. 85(Pt 5): p. 1153-65.

[65] Olmsted, R.A. and P.L. Collins, *The 1A protein of respiratory syncytial virus is an integral membrane protein present as multiple, structurally distinct species.* J Virol, 1989. 63(5): p. 2019-29.

[66] Collins, P.L. and G. Mottet, *Membrane orientation and oligomerization of the small hydrophobic protein of human respiratory syncytial virus.* J Gen Virol, 1993. 74 (Pt 7): p. 1445-50.

[67] Parthasarathy, K., et al., *Expression and purification of coronavirus envelope proteins using a modified β-barrel construct.* Protein Expression and Purification, 2012. 85(1): p. 133-141.

[68] Rixon, H.W., et al., *The respiratory syncytial virus small hydrophobic protein is phosphorylated via a mitogen-activated protein kinase p38-dependent tyrosine kinase activity during virus infection.* J Gen Virol, 2005. 86(Pt 2): p. 375-84.

[69] Gan, S.W., et al., *Structure and ion channel activity of the human respiratory syncytial virus (hRSV) small hydrophobic protein transmembrane domain.* Protein Sci., 2008. 17: p. 813-820.

[70] Carter, S.D., et al., *Direct visualization of the small hydrophobic protein of human respiratory syncytial virus reveals the structural basis for membrane permeability.* FEBS Letters, 2010. 584(13): p. 2786-2790.

[71] Gan, S.-W., et al., *The Small Hydrophobic Protein of the Human Respiratory Syncytial Virus Forms Pentameric Ion Channels.* Journal of Biological Chemistry, 2012. 287(29): p. 24671-24689.

[72] Gonzalez, J.M., et al., *A comparative sequence analysis to revise the current taxonomy of the family Coronaviridae.* Arch Virol, 2003. 148(11): p. 2207-2235.

[73] Siddell, S.G., *The Coronaviridae; an introduction*1995: Plenum Press, New York, N.Y.

[74] Enjuanes, L., et al., *Coronaviridae*, in *Virus taxonomy. Classification and nomenclature of viruses.*, M.H.V. van Regenmortel, et al., Editors. 2000, Academic Press: San Diego. p. 835-849.

[75] Gorbalenya, A.E., E.J. Snijder, and W.J. Spaan, *Severe acute respiratory syndrome coronavirus phylogeny: toward consensus.* J. Virol., 2004. 78(15): p. 7863-6.

[76] Hon, C.C., et al., *Evidence of the recombinant origin of a bat severe acute respiratory syndrome (SARS)-like coronavirus and its implications on the direct ancestor of SARS coronavirus.* J. Virol., 2008. 82(4): p. 1819-26.

[77] Vijgen, L., et al., *Complete genomic sequence of human coronavirus OC43: molecular clock analysis suggests a relatively recent zoonotic coronavirus transmission event.* J. Virol., 2005. 79(3): p. 1595-604.

[78] Lin, J.T., et al., *Safety and immunogenicity from a phase I trial of inactivated severe acute respiratory syndrome coronavirus vaccine.* Antivir Ther, 2007. 12(7): p. 1107-13.

[79] Barnard, D.L., et al., *Enhancement of the infectivity of SARS-CoV in BALB/c mice by IMP dehydrogenase inhibitors, including ribavirin.* Antiviral Res, 2006. 71(1): p. 53-63.

[80] Loutfy, M.R., et al., *Interferon alfacon-1 plus corticosteroids in severe acute respiratory syndrome: a preliminary study.* JAMA, 2003. 290(24): p. 3222-8.

[81] Keyaerts, E., et al., *In vitro inhibition of severe acute respiratory syndrome coronavirus by chloroquine.* Biochem Biophys Res Commun, 2004. 323(1): p. 264-8.

[82] Wu, C.J., et al., *Inhibition of severe acute respiratory syndrome coronavirus replication by niclosamide.* Antimicrob Agents Chemother, 2004. 48(7): p. 2693-6.

[83] Chen, F., et al., *In vitro susceptibility of 10 clinical isolates of SARS coronavirus to selected antiviral compounds.* J Clin Virol, 2004. 31(1): p. 69-75.

[84] Amici, C., et al., *Indomethacin has a potent antiviral activity against SARS coronavirus.* Antivir Ther, 2006. 11(8): p. 1021-30.

[85] Stockman, L.J., R. Bellamy, and P. Garner, *SARS: systematic review of treatment effects.* PLoS medicine, 2006. 3(9): p. e343.

[86] Cheng, P.W., et al., *Antiviral effects of saikosaponins on human coronavirus 229E in vitro.* Clin. Exp. Pharmacol. Physiol., 2006. 33(7): p. 612-6.

[87] Pyrc, K., et al., *Inhibition of human coronavirus NL63 infection at early stages of the replication cycle.* Antimicrob Agents Chemother, 2006. 50(6): p. 2000-8.

[88] Godet, M., et al., *TGEV corona virus ORF4 encodes a membrane protein that is incorporated into virions.* Virology, 1992. 188(2): p. 666-75.

[89] Liu, D.X. and S.C. Inglis, *Association of the infectious-bronchitis virus-3c protein with the virion envelope.* Virology, 1991. 185(2): p. 911-917.

[90] Yu, X., et al., *Mouse hepatitis-virus gene 5b protein is a new virion envelope protein.* Virology, 1994. 202(2): p. 1018-1023.

[91] Kall, L., A. Krogh, and E.L. Sonnhammer, *Advantages of combined transmembrane topology and signal peptide prediction--the Phobius web server.* Nucleic Acids Res., 2007. 35(Web Server issue): p. W429-32.

[92] Maeda, J., et al., *Membrane topology of coronavirus E protein.* Virology, 2001. 281(2): p. 163-169.

[93] Corse, E. and C.E. Machamer, *Infectious bronchitis virus E protein is targeted to the Golgi complex and directs release of virus-like particles.* J. Virol., 2000. 74(9): p. 4319-4326.

[94]   Yuan, Q., et al., *Biochemical evidence for the presence of mixed membrane topologies of the Severe Acute Respiratory Syndrome coronavirus envelope protein expressed in mammalian cells.* FEBS Lett., 2006. 580: p. 3192-3200.

[95]   Nieto-Torres, J.L., et al., *Subcellular location and topology of severe acute respiratory syndrome coronavirus envelope protein.* Virology, 2011. 415(2): p. 69-82.

[96]   Corse, E. and C.E. Machamer, *Infectious bronchitis virus E protein is targeted to the Golgi complex and directs release of virus-like particles.* J Virol, 2000. 74(9): p. 4319-26.

[97]   Maeda, J., et al., *Membrane topology of coronavirus E protein.* Virology, 2001. 281(2): p. 163-9.

[98]   Corse, E. and C.E. Machamer, *The cytoplasmic tail of infectious bronchitis virus E protein directs Golgi targeting.* J. Virol., 2002. 76(3): p. 1273-1284.

[99]   Lopez, L.A., et al., *Importance of conserved cysteine residues in the coronavirus envelope protein.* J. Virol., 2008. 82(6): p. 3000-3010.

[100] Boscarino, J.A., et al., *Envelope protein palmitoylations are crucial for murine coronavirus assembly.* J. Virol., 2008. 82(6): p. 2989-99.

[101] Thorp, E.B., et al., *Palmitoylations on murine coronavirus spike proteins are essential for virion assembly and infectivity.* J. Virol., 2006. 80(3): p. 1280-9.

[102] Kuo, L., K.R. Hurst, and P.S. Masters, *Exceptional flexibility in the sequence requirements for coronavirus small envelope protein function.* J. Virol., 2007. 81(5): p. 2249-62.

[103] Lim, K.P. and D.X. Liu, *The missing link in coronavirus assembly - Retention of the avian coronavirus infectious bronchitis virus envelope protein in the pre-Golgi compartments and physical interaction between the envelope and membrane proteins.* Journal of Biological Chemistry, 2001. 276(20): p. 17515-17523.

[104] Nal, B., et al., *Differential maturation and subcellular localization of severe acute respiratory syndrome coronavirus surface proteins S, M and E.* Journal of General Virology, 2005. 86: p. 1423-1434.

[105] Raamsman, M.J.B., et al., *Characterization of the coronavirus mouse hepatitis virus strain A59 small membrane protein E.* Journal of Virology, 2000. 74(5): p. 2333-2342.

[106] Cohen, J.R., L.D. Lin, and C.E. Machamer, *Identification of a Golgi Complex-Targeting Signal in the Cytoplasmic Tail of the Severe Acute Respiratory Syndrome Coronavirus Envelope Protein.* Journal of Virology, 2011. 85(12): p. 5794-5803.

[107] DeDiego, M.L., et al., *A severe acute respiratory syndrome coronavirus that lacks the E gene is attenuated in vitro and in vivo.* J. Virol., 2007. 81(4): p. 1701-13.

[108] Dediego, M.L., et al., *Pathogenicity of severe acute respiratory coronavirus deletion mutants in hACE-2 transgenic mice.* Virology, 2008. 376(2): p. 379-89.

[109] Netland, J., et al., *Immunization with an attenuated severe acute respiratory syndrome coronavirus deleted in E protein protects against lethal respiratory disease.* Virology, 2010. 399(1): p. 120-128.

[110] DeDiego, M.L., et al., *Severe acute respiratory syndrome coronavirus envelope protein regulates cell stress response and apoptosis.* PLoS Path., 2011. 7(10): p. e1002315.

[111] Bos, E.C., et al., *The production of recombinant infectious DI-particles of a murine coronavirus in the absence of helper virus.* Virology, 1996. 218(1): p. 52-60.

[112] Vennema, H., et al., *Nucleocapsid-independent assembly of coronavirus-like particles by co-expression of viral envelope protein genes.* EMBO Journal., 1996. 15(8): p. 2020-2028.

[113] Baudoux, P., et al., *Coronavirus pseudoparticles formed with recombinant M and E proteins induce alpha interferon synthesis by leukocytes.* J. Virol., 1998. 72(11): p. 8636-8643.

[114] Corse, E. and C.E. Machamer, *The cytoplasmic tails of infectious bronchitis virus E and M proteins mediate their interaction.* Virology, 2003. 312(1): p. 25-34.

[115] Mortola, E. and P. Roy, *Efficient assembly and release of SARS coronavirus-like particles by a heterologous expression system.* FEBS Lett., 2004. 576(1-2): p. 174-8.

[116] Fischer, F., et al., *Analysis of constructed E gene mutants of mouse hepatitis virus confirms a pivotal role for E protein in coronavirus assembly.* J. Virol., 1998. 72(10): p. 7885-7894.

[117] Curtis, K.M., B. Yount, and R.S. Baric, *Heterologous gene expression from transmissible gastroenteritis virus replicon particles.* J. Virol., 2002. 76(3): p. 1422-34.

[118] Ortego, J., et al., *Generation of a replication-competent, propagation-deficient virus vector based on the transmissible gastroenteritis coronavirus genome.* J. Virol., 2002. 76(22): p. 11518-29.

[119] Lim, K.P. and D.X. Liu, *The missing link in coronavirus assembly. Retention of the avian coronavirus infectious bronchitis virus envelope protein in the pre-Golgi compartments and physical interaction between the envelope and membrane proteins.* J. Biol. Chem., 2001. 276(20): p. 17515-17523.

[120] Yang, Y., et al., *Bcl-xL inhibits T-cell apoptosis induced by expression of SARS coronavirus E protein in the absence of growth factors.* Biochem. J., 2005. 392(1): p. 135-143.

[121] Alvarez, E., et al., *The envelope protein of severe acute respiratory syndrome coronavirus interacts with the non-structural protein 3 and is ubiquitinated.* Virology, 2010. 402(2): p. 281-91.

[122] Yoshikawa, T., et al., *Severe acute respiratory syndrome (SARS) coronavirus-induced lung epithelial cytokines exacerbate SARS pathogenesis by modulating intrinsic functions of monocyte-derived macrophages and dendritic cells.* J. Virol., 2009. 83(7): p. 3039-48.

[123] Madan, V., et al., *Viroporin activity of murine hepatitis virus E protein.* FEBS Lett., 2005. 579(17): p. 3607-12.

[124] Wilson, L., et al., *SARS coronavirus E protein forms cation-selective ion channels.* Virology, 2004. 330(1): p. 322-31.

[125] Wilson, L., P. Gage, and G. Ewart, *Hexamethylene amiloride blocks E protein ion channels and inhibits coronavirus replication.* Virology, 2006. 353(2): p. 294-306.

[126] Torres, J., et al., *Conductance and amantadine binding of a pore formed by a lysine-flanked transmembrane domain of SARS coronavirus envelope protein.* Protein Sci., 2007. 16(9): p. 2065-2071.

[127] Parthasarathy, K., et al., *Structural flexibility of the pentameric SARS coronavirus envelope protein ion channel.* Biophys. J., 2008. 95(6): p. L39-41.

[128] Verdia-Baguena, C., et al., *Coronavirus E protein forms ion channels with functionally and structurally-involved membrane lipids.* Virology, 2012. 432(2): p. 485-94.

[129] McBride, C.E. and C.E. Machamer, *Palmitoylation of SARS-CoV S protein is necessary for partitioning into detergent-resistant membranes and cell-cell fusion but not interaction with M protein.* Virology. 405(1): p. 139-48.

[130] Torres, J., et al., *Model of a putative pore: the pentameric α-helical bundle of SARS coronavirus E protein in lipid bilayers.* Biophys. J., 2006. 91: p. 938-947.

[131] Moore, W.H. and S. Krimm, *Vibrational analysis of peptides, polypeptides, and proteins. II. beta-poly(L-alanine) and beta-poly(L-anaylglycine).* Biopolymers, 1976. 15(12NA-NA-770103-770104): p. 2465-83.

[132] Moore, W.H. and S. Krimm, *Transition dipole coupling in Amide I modes of betapolypeptides.* Proc. Nat. Acad. Sci. USA, 1975. 72(12): p. 4933-4935.

[133] Krimm, S. and J. Bandekar, *Vibrational spectroscopy and conformation of peptides, polypeptides, and proteins.* Adv.Protein Chem., 1986. 38: p. 181-364.

[134] Byler, D.M. and H. Susi, *Examination of the secondary structure of proteins by deconvolved FTIR spectra.* Biopolymers, 1986. 25(3): p. 469-487.

[135] Torii, H. and M. Tasumi, *Model-Calculations on the Amide-I Infrared Bands of Globular-Proteins.* J. Chem. Phys., 1992. 96(5): p. 3379-3387.

[136] Combet, C., et al., *NPS@: network protein sequence analysis.* Trends Biochem Sci, 2000. 25(3): p. 147-50.

[137] Halverson, K., et al., *Molecular determinants of amyloid deposition in Alzheimer's disease: conformational studies of synthetic beta-protein fragments.* Biochemistry, 1990. 29(11): p. 2639-44.

[138] Kadurin, I., S. Huber, and S. Grunder, *A single conserved proline residue determines the membrane topology of stomatin.* Biochem. J., 2009. 418: p. 587-594.

[139] Kheterpal, I. and R. Wetzel, *Hydrogen/deuterium exchange mass spectrometry--a window into amyloid structure.* Acc Chem Res, 2006. 39(9): p. 584-93.

[140] Williams, A.D., et al., *Structural properties of Abeta protofibrils stabilized by a small molecule.* Proc. Nat. Acad. Sci. USA, 2005. 102(20): p. 7115-20.

[141] Nguyen, J.T., et al., *X-ray diffraction of scrapie prion rods and PrP peptides.* J. Mol. Biol., 1995. 252(4): p. 412-22.

[142] Geisler, N., et al., *Peptides from the conserved ends of the rod domain of desmin disassemble intermediate filaments and reveal unexpected structural features: a circular dichroism, Fourier transform infrared, and electron microscopic study.* J. Struct. Biol., 1993. 110(3): p. 205-14.

[143] Kreplak, L. and U. Aebi, *From the polymorphism of amyloid fibrils to their assembly mechanism and cytotoxicity.* Adv Protein Chem, 2006. 73: p. 217-33.

[144] Arfmann, H.A., R. Labitzke, and K.G. Wagner, *Conformational properties of L-leucine, L-isoleucine, and L-norleucine side chains in L-lysine copolymers.* Biopolymers, 1977. 16(8): p. 1815-26.

[145] Mutter, M., et al., *Sequence-dependence of secondary structure formation: conformational studies of host-guest peptides in alpha-helix and beta-structure supporting media.* Biopolymers, 1985. 24(6): p. 1057-74.

[146] Lopez de la Paz, M. and L. Serrano, *Sequence determinants of amyloid fibril formation.* Proc. Nat. Acad. Sci. USA, 2004. 101(1): p. 87-92.

[147] Hernandez, L.D. and J.M. White, *Mutational analysis of the candidate internal fusion peptide of the avian leukosis and sarcoma virus subgroup a envelope glycoprotein.* J. Virol., 1998. 72(4): p. 3259-3267.

[148] Ito, H., et al., *Mutational analysis of the putative fusion domain of Ebola virus glycoprotein.* J. Virol., 1999. 73(10): p. 8907-12.

[149] Wolfsberg, T.G., et al., *ADAM, a widely distributed and developmentally regulated gene family encoding membrane proteins with a disintegrin and metalloprotease domain.* Dev. Biol., 1995. 169(1): p. 378-83.

[150] Tugarinov, V., et al., *A cis proline turn linking two beta-hairpin strands in the solution structure of an antibody-bound HIV-1IIIB V3 peptide.* Nat Struct Biol, 1999. 6(4): p. 331-5.

[151] Pedersen, J.S. and D.E. Otzen, *Amyloid-a state in many guises: survival of the fittest fibril fold.* Protein Sci., 2008. 17(1): p. 2-10.

[152] Fandrich, M., M.A. Fletcher, and C.M. Dobson, *Amyloid fibrils from muscle myoglobin.* Nature, 2001. 410(6825): p. 165-6.

[153] Guijarro, J.I., et al., *Amyloid fibril formation by an SH3 domain.* Proceedings of the National Academy of Sciences of the United States of America, 1998. 95(8): p. 4224-8.

[154] Munch, J., et al., *Semen-derived amyloid fibrils drastically enhance HIV infection.* Cell, 2007. 131(6): p. 1059-71.